Available online at www.sciencedirect.com
ScienceDirect
Journal of Theoretical Biology 245 (2007) 627–637
Journal of Theoretical Biology
www.elsevier.com/locate/yjtbi

Stochastic Markovian modeling of electrophysiology of ion channels: Reconstruction of standard deviations in macroscopic currents

Sarah E. Geneser[a], Robert M. Kirby[a], Dongbin Xiu[b], Frank B. Sachse[c,*]

[a]School of Computing, University of Utah, Salt Lake City, UT 84112, USA
[b]Department of Mathematics, Purdue University, West Lafayette, IN 47907, USA
[c]Nora Eccles Harrison Cardiovascular Research and Training Institute, University of Utah, Salt Lake City, UT 84112, USA

Received 21 April 2006; received in revised form 31 August 2006; accepted 16 October 2006
Available online 20 October 2006

Abstract

Markovian models of ion channels have proven useful in the reconstruction of experimental data and prediction of cellular electrophysiology. We present the stochastic Galerkin method as an alternative to Monte Carlo and other stochastic methods for assessing the impact of uncertain rate coefficients on the predictions of Markovian ion channel models. We extend and study two different ion channel models: a simple model with only a single open and a closed state and a detailed model of the cardiac rapidly activating delayed rectifier potassium current. We demonstrate the efficacy of stochastic Galerkin methods for computing solutions to systems with random model parameters. Our studies illustrate the characteristic changes in distributions of state transitions and electrical currents through ion channels due to random rate coefficients. Furthermore, the studies indicate the applicability of the stochastic Galerkin technique for uncertainty and sensitivity analysis of bio-mathematical models.

Keywords: Stochastic Galerkin; Polynomial chaos; Stochastic processes; Markov modeling; Ion channels

1. Introduction

Ion channels are pore-forming proteins that permit and control the diffusion of ions across cellular membranes (Hille, 2001). They are the object of intensive research, both from the experimental as well as the mathematical perspective. As a consequence of this emphasis, various approaches exist to mathematically model ion channel behavior. Prior to the experimental verification of ion channel existence, models were already utilized to predict membrane response and the mechanisms underlying channel behavior. Such models are now ubiquitous in the ion channel research community.

Most mathematical electrophysiological models of ion channels fall into one of two categories: Markovian or Hodgkin–Huxley type. Markovian models describe ion channel behavior by assigning probabilities to potential channel states such as open, inactive, and closed states (Colquhoun and Hawkes, 1995a). Transitions between the states are governed by rate coefficients which are a function of physical parameters, e.g. temperature, transmembrane voltage and ion concentrations. Hodgkin–Huxley type models of ion channels follow a mathematical formalism introduced in the seminal work of Hodgkin and Huxley for describing the electrophysiology of membrane of a squid axon (Hodgkin and Huxley, 1952). Kinetics of channel properties are described by coefficients, which are dependent on time and physical parameters. The coefficients affect the current flow through channels in a multiplicative manner.

The traditional experimental approach for investigating and quantifying ion channel behavior involves the simultaneous application of voltage clamping protocols and measurement of the resulting electrical currents through either single or multiple membrane embedded ion channels. Ion channel modeling has proven to be a valuable addition to the experimental methodology and is capable of

*Corresponding author. Tel.: +1 801 587 9514; fax: +1 801 581 3128.
E-mail addresses: geneser@cs.utah.edu (S.E. Geneser), kirby@cs.utah.edu (R.M. Kirby), dxiu@math.purdue.edu (D. Xiu), fs@cvrti.utah.edu (F.B. Sachse).

0022-5193/$ - see front matter © 2006 Elsevier Ltd. All rights reserved.
doi:10.1016/j.jtbi.2006.10.016

reconstructing experimental data and providing mechanistic insights into physiological and pathophysiological phenomena (Hodgkin and Huxley, 1952; McAllister et al., 1975; Luo and Rudy, 1991; Rudy, 2004; Sachse, 2004).

Noise in the current response of electrically active membranes can be categorized as either thermal or so-called excess noise (Verveen and DeFelice, 1974). Excess noise has been proposed to result from the granular ion current transport through channel pores, ion–ion interaction, and stochastic conformational changes of the channels such as their opening and closing. Further sources of fluctuations, particularly in macroscopic currents through ensembles of ion channels, may originate from the heterogeneity of kinetic properties and local variations in physical conditions in the channel vicinity.

Analysis of macroscopic current noise and single channel stochasticity provides significant biophysical insights and is an important tool for modeling (Colquhoun and Hawkes, 1995a, b; Colquhoun and Sigworth, 1995). However, ion channel models typically neglect noise and describe only the average behavior. Rather than computing a spread of outcomes resulting from randomly distributed input data and/or model parameters, these models produce a single result for deterministic input data and model parameters. While such simplifications are appropriate for certain systems, they render the model incapable of reconstructing heterogeneous behavior of channels. These restrictions can significantly reduce the insights to be gained from computational simulations.

In this paper, we assume Markovian models of ion channel electrophysiology and investigate the stochastic state dynamics and current response to randomly distributed rate coefficients. The approach aims at assessing current noise resulting from heterogeneity of kinetic channel properties and physical conditions in the channel vicinity.

A common method of investigating the effects of random parameters involves simulating the model multiple times, each with different values for the rate coefficients (varied individually or in combination). The current responses to each set of rate coefficients can then be compared to obtain an understanding of the effect of the rate coefficients. This is similar to taking specific realizations from a randomly distributed rate constant and using those values to run the deterministic model. From these discrete results, one can calculate an estimate of the response statistics, e.g. the mean and variance. As one increases the number of samples, the solution statistics converge. Such an approach falls under the category of sampling-based stochastic methods.

Requiring only a straightforward extension of the deterministic solver, Monte Carlo methods are the best known of these techniques due to their ease of implementation. However, such solutions are often computationally prohibitive even for systems of relatively low complexity, as they converge as $1/\sqrt{N}$ where N is the number of realizations. Thus a large number of trials are necessary to obtain accurate statistics. Latin hypercube sampling (Loh, 1996), the quasi-Monte Carlo method (Niederreiter et al., 1998), and the Markov chain Monte Carlo method (Gamerman, 1997) all have accelerated convergence properties compared to the Monte Carlo method while maintaining ease of implementation. However, each method imposes certain restrictions on the process of interest which in turn limits their general applicability.

An alternative method to determine the effect of rate coefficient values upon a particular ion channel model is to assume a probability density function and directly calculate the current as a result of the (now) stochastic ion channel model. Such non-sampling methods avoid taking large samples of repetitive deterministic solvers and include perturbation methods (Kleiber and Hein, 1992) and second-moment analysis (Liu et al., 1986). Though more efficient than Monte Carlo under certain conditions, these methods have limited utility and robustness as they are only capable of resolving relatively small perturbations in both the random inputs and outputs. This is difficult to guarantee, especially for nonlinear systems where small perturbations in inputs can result in relatively large perturbations in the response.

In this paper, we adopt the generalized polynomial chaos–stochastic Galerkin (gPC–SG) method as an efficient computational means of obtaining solutions to complex stochastic differential systems. Generalized polynomial chaos (gPC) represents random processes via orthogonal polynomials (Xiu and Karniadakis, 2002a, b). It is a generalization of the Wiener-Hermite polynomial chaos expansion (Wiener, 1938)[1] which employs Hermite polynomials. The generalizations utilize sets of orthogonal polynomials to allow efficient representation of random processes with arbitrary probability distribution functions. Such expansions exhibit fast convergence rates when the stochastic response of the system is sufficiently smooth in the random space.

The traditional approach involves a Galerkin projection of the governing equations to the random polynomial basis functions defined by gPC, such that the mean square error of the residue is minimized. This is referred to as the stochastic Galerkin method, which efficiently reduces the stochastic governing equations to a system of deterministic equations that can be solved by conventional numerical techniques. Such a gPC–SG approach is capable of resolving systems with relatively large perturbations in both the inputs and responses and has been successfully applied to model uncertainty in complex stochastic solid and fluid dynamic problems (Ghanem and Spanos, 1991; Xiu and Karniadakis, 2002a, b; Xiu and Karniadakis,

[1]The term "polynomial chaos" was designated by Wiener in his 1938 seminal paper, long before the field of dynamical chaos theory became popular.

2003). However, the resulting deterministic equations can become very complicated and potentially intractable if the system of differential equations has nontrivial and/or nonlinear forms. Such difficulties are not typical of Markovian ion channel models which we study in this paper.

In this work we employ the gPC–SG method to assess the impact of rate coefficients on computational simulations of cardiac ion channel phenomena. We seek a quantitative understanding of the relationship between the distributions of rate coefficients and ion channel currents as a result of deterministic voltage clamping protocol. We first consider a simple Markovian model of ion channel behavior, and then apply our technique to a cardiac ion channel model of the slowly activating delayed rectifier potassium current, I_{Kr} (Iyer et al., 2004). While we only consider random rate coefficients in ion channel models, this methodology can be applied to other parameters, and, furthermore, a vast number of bio-mathematical models.

2. Stochastic Galerkin application

2.1. Generalized polynomial chaos expansion

We first briefly demonstrate the application of gPC to a general stochastic process with N independent parameters. To assess the impact of each of these parameters, we model them as random variables and assume that they are functions of N separate, independent and uncorrelated random variables, denoted $(\boldsymbol{\xi}) = (\xi_1, \xi_2, \ldots, \xi_N)$. The output of the system, $f(\boldsymbol{\xi})$, is dependent on the parameters and is therefore also a random process. Utilizing gPC expansions, such a process is approximated by a linear combination of orthogonal polynomials, $\phi(\boldsymbol{\xi})$ as follows:

$$f(\boldsymbol{\xi}) \approx \sum_{i=0}^{\infty} \hat{f}_i \phi_i(\boldsymbol{\xi}), \tag{1}$$

$$\hat{f}_i = \int_{-\infty}^{\infty} f(\boldsymbol{\xi})\phi_i(\boldsymbol{\xi})\,\mathrm{d}\mu = \int_{-\infty}^{\infty} w(\boldsymbol{\xi}) f(\boldsymbol{\xi})\phi_i(\boldsymbol{\xi})\,\mathrm{d}\boldsymbol{\xi}, \tag{2}$$

where $\hat{f}_i$ is a projection of the process against the ith polynomial, μ and $w(\boldsymbol{\xi})$ denote the probability measure and probability density function associated with the probability of the chosen polynomial basis functions. It has been shown that optimal convergence can be achieved by choosing the gPC type of orthogonal polynomials based on the probability distribution of the input parameters, e.g. Hermite polynomials are more appropriate for the Gaussian distribution, Legendre for uniform, etc. (Xiu and Karniadakis, 2002a, b). The general expression for the Legendre polynomials is given by

$$L_n(\xi_1, \ldots, \xi_N) = (2^n n!)^{-1} \frac{\partial^n}{\partial\xi_1 \ldots \partial\xi_N}[(\boldsymbol{\xi}^{\mathrm{T}}\boldsymbol{\xi} - 1)^n]. \tag{3}$$

The Legendre polynomials as a function of a single random variable, ξ are

$$\phi_0(\xi) = 1, \quad \phi_1(\xi) = \xi, \quad \phi_2(\xi) = \tfrac{1}{2}(3\xi^2 - 1),$$
$$\phi_3(\xi) = \tfrac{1}{2}(5\xi^3 - 3\xi), \ldots \tag{4}$$

and are applied in the gPC–SG solutions of the systems described in Sections 2.2 and 2.3.

2.2. Simple Markovian model

We first illustrate the application of the stochastic Galerkin representation to compute the response of a simple Markovian model of ion channels to stochastically distributed rate coefficients. The model mimics the behavior of unspecified ion channels as a two-state process with a single open and closed state with state the transition dynamics depicted in Fig. 1a. The deterministic current response of this system is described by the following system of differential equations:

$$I(t) = \bar{G}O(t)(V(t) - E_K), \tag{5}$$

$$\frac{\mathrm{d}C(t)}{\mathrm{d}t} = -\alpha(V)C(t) + \beta(V)O(t), \tag{6}$$

$$\frac{\mathrm{d}O(t)}{\mathrm{d}t} = -\beta(V)O(t) + \alpha(V)C(t), \tag{7}$$

where O and C denote the probability an ion channel is in the open or closed state, respectively. $V(t)$ is the voltage across the cell membrane, and $\alpha(V) = \alpha_m e^{\alpha_e V}$ and $\beta(V) = \beta_m e^{\beta_e V}$ are the rate coefficients for state transitions. $I(t)$ denotes the electrical current through the channels. Further constants and parameters are given in Tables 1 and 2.

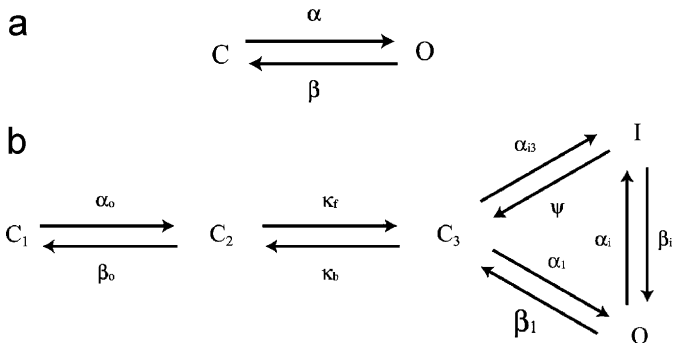

Fig. 1. State diagram for (a) simple and (b) I_{Kr} model.

Table 1
Physical quantities and constants

Name	Symbol	Value
Temperature	T	293.00 K
Faraday's constant	F	96.485 °C m mol^{-1}
Gas constant	R	8.3144 J mol^{-1} K^{-1}
Potassium reversal potential	E_K	87.027 mV

Table 2
Parameters and initial conditions for the simple model

Name	Symbol	Mean value
Summary channel conductance	$\bar{G}$	$0.2\,\mathrm{mS/\mu F}$
Initial close probability	$C(t=0)$	7.07×10^{-1}
Initial open probability	$O(t=0)$	2.93×10^{-1}
Rate constant (function of voltage V)	α	$4.0\times10^{-2}e^{1.0\times10^{-2}\,\mathrm{V}}\,\mathrm{m\,s^{-1}}$
Rate constant (function of voltage V)	β	$1.0\times10^{-2}e^{-1.0\times10^{-2}\,\mathrm{V}}\,\mathrm{m\,s^{-1}}$
Concentration of extracellular potassium	$[K^+]_o$	4.0 mM
Concentration of intracellular potassium	$[K^+]_i$	$1.256\times10^{2}\,\mathrm{mM}$

Markovian ion channel models assume that the law of large numbers applies to the ion channel system in question and model its mean behavior responses. In discussing randomness or stochasticity in the following text, we are not referring to this aspect of the models. Instead, we investigate the effect of introducing random parameters to Markovian models.

The above system is deterministic and can be solved using the typical numerical methods for ordinary differential systems, such as the Euler and Runge-Kutta methods (Hairer et al., 1993). We now consider the response of the system when the rate coefficient multiplicative term α_m is random, and has a given probability density function. Because α_m is a random process, α is also random, and the probability density function is also known.

We first choose the appropriate basis polynomials for the given probability density function of the rate constant, $\alpha(\xi)$. For example, if $\alpha(\xi)$ is assumed to be a uniform random process with given mean, η, and half interval length, σ: utilizing Legendre polynomials for the basis, $\phi(\xi)$, the representation simplifies to $\alpha(\xi)=\hat{\alpha}_0\phi_0(\xi)+\hat{\alpha}_0\phi_1(\xi)+\cdots+\hat{\alpha}_P\phi_P(\xi)=\eta+\sigma\xi$. This simplification occurs because in the case of a uniform process, the first mode, $\hat{\alpha}_0$ is η, the second mode, $\hat{\alpha}_1$, is σ, and only linear Legendre polynomials are required to fully represent a uniform process. This framework is valid for random processes with any underlying probability distribution function.

We then decompose the remaining stochastic functions into weighted sums of the $P+1$ polynomial basis functions as follows:

$$\alpha(\xi)=\eta+\sigma\xi, \tag{8}$$

$$I(t;\xi)=\sum_{j=0}^{P}\hat{I}_j(t)\phi_j(\xi), \tag{9}$$

$$O(t;\xi)=\sum_{k=0}^{P}\hat{O}_k(t)\phi_k(\xi), \tag{10}$$

$$C(t;\xi)=\sum_{l=0}^{P}\hat{C}_l(t)\phi_l(\xi), \tag{11}$$

where η and σ are known, and $\hat{I}_j$, $\hat{O}_k$, and $\hat{C}_l$ $(j,k,l=0\ldots P)$ must be computed. The numerical accuracy improves with increased expansion order, p, and the number of polynomials necessary for the expansion is $P=(N+p)!/N!p!-1$ where N is the number of random variables. This number can become computationally intractable for large N, and as such, we restrict the experiments presented here to two uncorrelated, independent random variables. Note that basis polynomials higher than linear are required for the representation of channel states and current, as they are not guaranteed to have uniform distributions due to the non-linear interactions of the model equations. The states and current are assumed to have non-random distributions at $t=0$, and their PDFs evolve from their initial probability density as a consequence of the stochastic differential operator.

For the stochastic Galerkin method, we chose the test functions to be identical to the polynomial basis, or trial functions. Substituting the representations of the current and states in Eqs. (8)–(11) and the representation of $\alpha(\xi)$ into the system and projecting against the test functions (which we take to be the basis polynomials), we obtain for each $m=0,\ldots,P$:

$$\sum_{j=0}^{P}\mathscr{M}_{mj}\hat{I}_j(t)=\bar{G}\sum_{k=0}^{P}\mathscr{M}_{mk}\hat{O}_k(t)(V(t)-E_K), \tag{12}$$

$$\frac{\mathrm{d}}{\mathrm{d}t}\sum_{l=0}^{P}\mathscr{M}_{ml}\hat{C}_l(t)=-\sum_{l=0}^{P}[\eta\mathscr{C}_{ml0}+\sigma\mathscr{C}_{ml1}]\hat{C}_l(t)+\beta\sum_{k=0}^{P}\mathscr{M}_{mk}\hat{O}_k(t), \tag{13}$$

$$\frac{\mathrm{d}}{\mathrm{d}t}\sum_{k=0}^{P}\mathscr{M}_{mk}\hat{O}_k(t)=-\beta\sum_{k=0}^{P}\mathscr{M}_{mk}\hat{O}_k(t)+\sum_{l=0}^{P}[\eta\mathscr{C}_{ml0}+\sigma\mathscr{C}_{ml1}]\hat{C}_l(t), \tag{14}$$

where $\mathscr{C}_{ijk}=\int_{\mathscr{S}}\phi_i(\xi)\phi_j(\xi)\phi_k(\xi)\,\mathrm{d}\mu$ and $\mathscr{M}_{ij}=\int_{\mathscr{S}}\phi_i(\xi)\phi_j(\xi)\,\mathrm{d}\mu$. One can compute these values by quadrature to populate the matrices $\mathscr{C}_0$ and $\mathscr{C}_1$ described in the following section. In this expression, $\mathscr{S}$ denotes the domain of

integration which is determined by the support of random variables $\boldsymbol{\xi}$. For example, for uniform random variables, $\mathscr{S} = [-1, 1]^N$.

This set of stochastic differential equations can be represented by the following matrix system:

$$\mathscr{C}_0 \boldsymbol{I}(t) = \bar{G}(V(t) - E_K)\mathscr{C}_0 \boldsymbol{O}(t), \tag{15}$$

$$\mathscr{C}_0 \frac{\mathrm{d}}{\mathrm{d}t} \boldsymbol{C}(t) = -[\eta \mathscr{C}_0 + \sigma \mathscr{C}_1]\boldsymbol{C}(t) + \beta \mathscr{C}_0 \boldsymbol{O}(t), \tag{16}$$

$$\mathscr{C}_0 \frac{\mathrm{d}}{\mathrm{d}t} \boldsymbol{O}(t) = -\beta \mathscr{C}_0 \boldsymbol{O}(t) + [\eta \mathscr{C}_0 + \sigma \mathscr{C}_1]\boldsymbol{C}(t), \tag{17}$$

where $\mathscr{C}_0$ and $\mathscr{C}_1$ are $(P+1)$ by $(P+1)$ matrices such that $(\mathscr{C}_0)_{ij} = \mathscr{C}_{0ij}$ and $(\mathscr{C}_1)_{ij} = \mathscr{C}_{1ij}$, and $\boldsymbol{I}$, $\boldsymbol{O}$, and $\boldsymbol{C}$ are vectors of size $P+1$ with $(\boldsymbol{I}(t))_i = \hat{I}_i(t)$, $(\boldsymbol{O}(t))_i = \hat{O}_i(t)$, and $(\boldsymbol{C}(t))_i = \hat{C}_i(t)$.

Due to the properties of the inner product and the basis, both $\mathscr{C}_0$ and $\mathscr{C}_1$ are symmetric positive definite, and thus invertible.

This system can further be simplified to

$$\boldsymbol{I}(t) = \bar{G}(V(t) - E_K)\boldsymbol{O}(t), \tag{18}$$

$$\frac{\mathrm{d}}{\mathrm{d}t} \boldsymbol{C}(t) = -[\eta + \sigma \mathscr{C}_0^{-1}\mathscr{C}_1]\boldsymbol{C}(t) + \beta \boldsymbol{O}(t), \tag{19}$$

$$\frac{\mathrm{d}}{\mathrm{d}t} \boldsymbol{O}(t) = -\beta \boldsymbol{O}(t) + [\eta + \sigma S \mathscr{C}_0^{-1}\mathscr{C}_1]\boldsymbol{C}(t) \tag{20}$$

which can also be solved via the typical numerical ODE solvers.

2.3. Markovian model of rapidly activating delayed rectifier K^+ current

We chose a model of the rapidly activating delayed rectifier K^+ current (I_{Kr}) in human ventricular subepicardial myocytes developed by Iyer et al. (2004) to investigate the reaction of a more complex ion channel model to random parameters.

The system of ordinary differential equations describing the behavior of the I_{Kr} channels is given by

$$I_{Kr} = \bar{G} O \sqrt{\frac{[\mathrm{K}^+]_o}{4}}(V - E_K), \tag{21}$$

$$\frac{\mathrm{d}C_1}{\mathrm{d}t} = -\alpha_0 C_1 + \beta_0 C_2, \tag{22}$$

$$\frac{\mathrm{d}C_2}{\mathrm{d}t} = -(\beta_0 + k_f)C_2 + \alpha_0 C_1 + k_b C_3, \tag{23}$$

$$\frac{\mathrm{d}C_3}{\mathrm{d}t} = -(\alpha_1 + \alpha_{i3} + k_b)C_3 + k_f C_2 + \beta_1 O + \Psi I, \tag{24}$$

$$\frac{\mathrm{d}I}{\mathrm{d}t} = -(\Psi + \beta_i)I + \alpha_{i3} C_3 + \alpha_i O, \tag{25}$$

$$\frac{\mathrm{d}O}{\mathrm{d}t} = -(\beta_1 + \alpha_i)O + \alpha_1 C_3 + \beta_i I. \tag{26}$$

The parameters and initial conditions are specified in Table 3. The state transitions are depicted in Fig. 1b.

For this system, the rate coefficients k_f and k_b are constant values, and all other rate coefficients are of the form $a^m e^{a^e V}$, consisting of a multiplicative factor, a^m, and an exponential factor, a^e.

We can allow any of the parameters to be stochastic in the model and apply gPC as described for the simple model. Even random parameters expressed as rational, trigonometric or exponential functions can be handled as one would normally accomplish Galerkin projections. To do this, one must project the non-linear function of random parameters onto the SG basis chosen for the system. In this case, the exact integrals in Galerkin projections are usually replaced by discrete (multivariate) integration rules, e.g. quadratures, with sufficient accuracy. We refer the reader to a standard reference on higher-order methods (Canuto et al., 1987) for further information concerning implementation of projections and quadrature.

3. Results

3.1. Simple Markovian model

We first present the simulated currents of the simple channel model for a given voltage clamping protocol (Table 4) with random rate coefficients of uniform distributions. The various computational results presented for this model assume the voltage clamping protocol shown in the insert of Fig. 2a. The mean current responses for all stochastic experiments presented for the simple model are nearly visually indistinguishable from the response to the deterministic model and are superimposed in Fig. 2a. The stochastic rate coefficients have little effect on the mean of the solution because the random spread of coefficient multiplier values affect the current nearly symmetrically about the deterministic solution.

The standard deviation of the current for the stochastic rate coefficient multiplier, $\alpha_m(\boldsymbol{\xi})$, with all other model parameters deterministic exhibits similar behavior to the standard deviation when only $\beta_m(\boldsymbol{\xi})$ is stochastic (Fig. 2b). In both cases, the maximum of the standard deviation are nearly the same. The standard deviation in both cases increases for $t \in [0, 2]$ s because the distribution of rate coefficients result in a distribution of equilibrium current for -60 mV. Additionally, the equilibrium values both reach for the various clamping voltages are very similar. However, the random β_m case reaches its maximum very quickly after the voltage jump at $t = 2$ s, while α_m is delayed in reaching its maximum standard deviation. Additionally, the elevation in standard deviation after $t = 2$ s is prolonged for $\alpha_m(\boldsymbol{\xi})$ as compared with $\beta_m(\boldsymbol{\xi})$. The decrease in voltage at $t = 4$ s results in a marked decrease in standard deviation for both cases.

When both rate coefficients are assumed to be stochastic functions of the same random variable (Fig. 2), the

Table 3
Parameters and initial conditions for the I_{Kr} model

Parameter	Symbol	Mean value
Summary channel conductance	$\bar{G}$	$0.0186\,\mathrm{mS/\mu F}$
Concentration of extracellular potassium	$[K^+]_o$	$4.0\,\mathrm{mM}$
Concentration of intracellular potassium	$[K^+]_i$	$1.256\times10^{2}\,\mathrm{mM}$
Initial probability	$C_1(t=0)$	9.967×10^{-1}
Initial probability	$C_2(t=0)$	4.341×10^{-4}
Initial probability	$C_3(t=0)$	7.634×10^{-5}
Initial probability	$I(t=0)$	1.533×10^{-6}
Initial probability	$O(t=0)$	9.512×10^{-6}
Rate constant (function of voltage V)	α_0	$0.0171e^{0.033\,V}\,\mathrm{m\,s^{-1}}$
Rate constant (function of voltage V)	β_0	$0.0397e^{-0.0431\,V}\,\mathrm{m\,s^{-1}}$
Rate constant (function of voltage V)	α_1	$0.0206e^{0.0262\,V}\,\mathrm{m\,s^{-1}}$
Rate constant (function of voltage V)	β_1	$0.0013e^{-0.0269\,V}\,\mathrm{m\,s^{-1}}$
Rate constant (function of voltage V)	α_i	$0.1067e^{0.0057\,V}\,\mathrm{m\,s^{-1}}$
Rate constant (function of voltage V)	β_i	$0.0065e^{-0.0454\,V}\,\mathrm{m\,s^{-1}}$
Rate constant (function of voltage V)	α_{i3}	$8.45\times10^{-5}e^{6.98\times10^{-7}\,V}\,\mathrm{m\,s^{-1}}$
Rate constant (function of voltage V)	Ψ	$\frac{\beta_1\beta_i\alpha_{i3}}{\alpha_1\alpha_i}$
Rate constant	k_f	$0.0261\,\mathrm{m\,s^{-1}}$
Rate constant	k_b	$0.1483\,\mathrm{m\,s^{-1}}$

Table 4
Voltage clamping protocols

Time interval	Voltage (mV)
Simple model protocol	
[0,2]	−60
(2,4]	−20
(4,5]	−60
I_{Kr} activation protocol	
[0,0.06]	−80
(0.06,2]	40
(2,3.9]	−70
(3.9,4]	−80
I_{Kr} inactivation protocol	
[0,0.06]	−80
(0.06,2.01]	40
(2.01,4.06]	−140
(4.06,4.12]	−80

behavior of the standard deviation is markedly different from that of the coefficients varying individually. The standard deviation is reduced overall and is zero from 0 to 2 s. This occurs because the rate coefficients are functions of the same random variable, ξ_1. In each realization of the stochastic distribution, the rate coefficient multipliers are perturbed from their mean value by the same percentage if the standard deviations of their distributions are the same percentage. We expect the equilibrium values of the current to be the same for all of the realizations of such a stochastic system, and thus the zero values in the standard deviation for $t\in[0,2]\,\mathrm{s}$ and $t=4\,\mathrm{s}$. We also observed a reduced overall standard deviation as compared to the two rate coefficients varying independently. In all experiments, the greatest standard deviation is observed just after $t=2\,\mathrm{s}$, when the mean current is rising fastest. This suggests that the rate coefficient values exhibit the greatest affect upon the speed of current increase.

When both are assumed to be stochastic functions of independent random variables, the realizations of rate coefficients $\alpha_m(\xi_1)$ and $\beta_m(\xi_2)$ are no longer tied to each other as for the previous example. The standard deviation shown in Fig. 2 appears to be more of a combination of the standard deviations resulting from the two coefficients varying individually. Also, the overall standard deviation in this case is higher than any of the other stochastic experiments with this model.

3.2. Markovian model of I_{Kr}

The standard deviations resulting from random uniform distributions for each I_{Kr} individual rate coefficient for both activation and inactivation voltage clamping protocols (Table 4) are grouped into several categories according to their qualitative behavior. The mean current responses for all the random parameters for the activation and inactivation protocol are superimposed in Figs. 3 and 8, respectively. As in the simplified model, the mean currents for most of the random experiments are not visually distinguishable with two exceptions. The random parameter $\alpha_i^m(\boldsymbol{\xi})$ results in an elevation in mean current for the activation protocol from $t=0\,\mathrm{s}$ while random $\beta_1^m(\boldsymbol{\xi})$ results in an elevation in the mean current for the same protocol from 2 s. The mean current responses for all random inactivation experiments are nearly indistinguishable from each other.

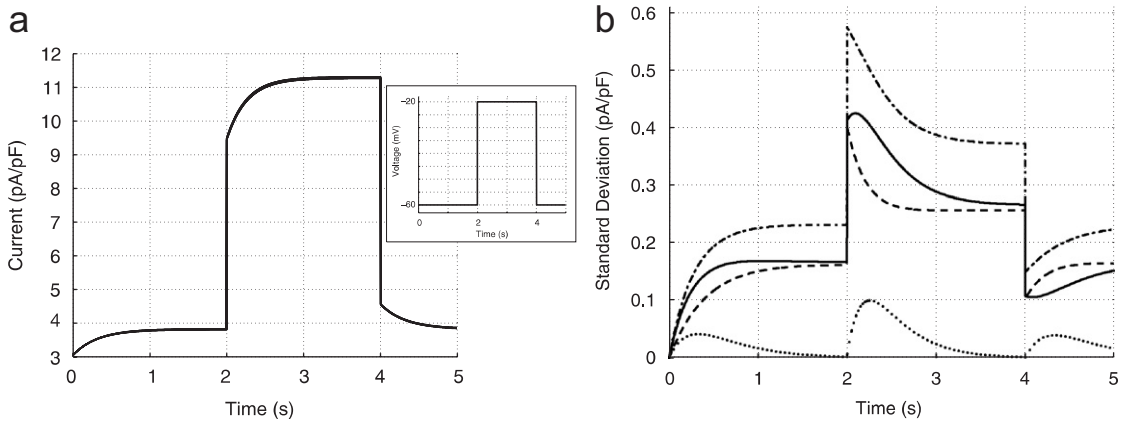

Fig. 2. Stochastic results for simple model with random α and β: (a) The mean currents are shown along with the insert of the applied voltage protocol. (b) The standard deviations are shown for random rate constant multiplier α_m (solid) and β_m (dashed), in case of both are functions of the same random variable, i.e. $\alpha_m(\xi_1)$ and $\beta_m(\xi_1)$ (dotted), and in case of α_m and β_m are functions of two separate, uncorrelated and independent random variables, i.e. $\alpha_m(\xi_1)$ and $\beta_m(\xi_2)$ (dash-dotted). For all of the experiments, the mean values of the rate coefficient multipliers are $\alpha_m = 4.00 \times 10^{-2}\,\mathrm{m\,s^{-1}}$ and $\beta_m = 5.00 \times 10^{-3}\,\mathrm{m\,s^{-1}}$. When given a stochastic distribution, $\alpha_m(\xi)$ is centered around $4.00 \times 10^{-2}\,\mathrm{m\,s^{-1}}$ and ranges uniformly from $\pm 50\%$ of the mean value, while β_m has a uniform distribution centered around $5.00 \times 10^{-3}\,\mathrm{m\,s^{-1}}$ and ranges from $\pm 50\%$.

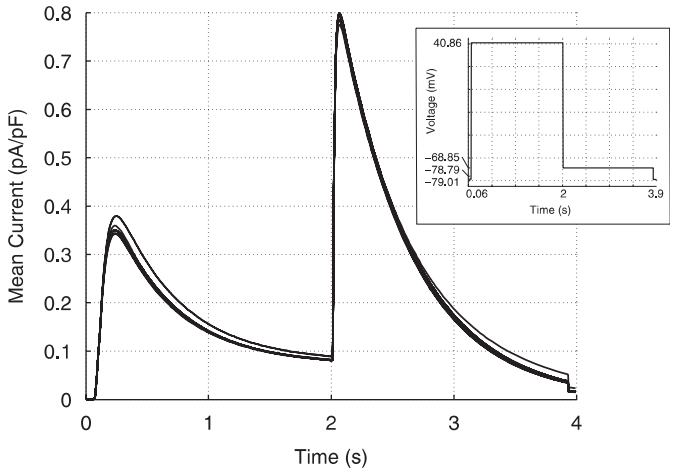

Fig. 3. Response of I_{Kr} model to activation: the mean current from the deterministic problem is similar to the currents of the various random experiments. The voltage clamping protocol is depicted in the insert.

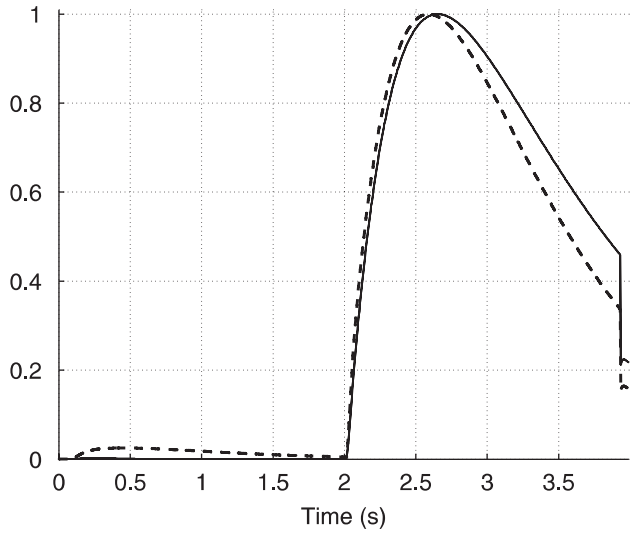

Fig. 4. Random β_1^m and α_{i3}^m response to activation: the normalized standard deviation of the current is shown for random rate coefficients β_1^m (solid) and α_{i3}^m (dashed). In both cases, the random rate coefficients have uniform distributions centered around their text values and ranging from $\pm 50\%$ of their mean value. The maximum values for the standard deviations are given in Table 5.

Random $\beta_1^m(\boldsymbol{\xi})$ and $\alpha_{i3}^m(\boldsymbol{\xi})$ (Figs. 4 and 9, Table 5) result in qualitatively similar standard deviations in current for both activation and inactivation protocols. The greatest effect is seen after $t = 2\,\mathrm{s}$, but the standard deviation shows a brief increase for the inactivation protocol as opposed to a more prolonged effect for the activation protocol. Maximum standard deviation values reached for both these random variables indicate that their impact is more pronounced for the inactivation protocol. This is not so surprising in the case of $\alpha_{i3}^m(\boldsymbol{\xi})$ as it controls the rate of change from the third closed state C_3 to the inactive state I and its effect upon channel inactivation is orders of magnitude greater than upon activation. Rate coefficient $\beta_1^m(\boldsymbol{\xi})$ controls the transfer from the open state O to the third closed state C_3.

Random $\alpha_0^m(\boldsymbol{\xi})$, $\beta_0^m(\boldsymbol{\xi})$, $\alpha_i^m(\boldsymbol{\xi})$, $k_f(\boldsymbol{\xi})$ and $k_b(\boldsymbol{\xi})$ give similar standard deviations in the current response (Figs. 5 and 10) to both protocols. For activation, the effect is most pronounced between $t = 0$ and 1 s. Here, we observe that the effect of these rate coefficient multipliers are stronger for the activation protocol than for inactivation, excepting the case of $\alpha_1^m(\boldsymbol{\xi})$, which regulates the transition from the third closed state C_3 to the open state O.

Table 5
Maximum standard deviations of the current in response to random rate coefficients for activation protocol

Random rate coefficient	Maximum standard deviation
α_0^m	4.14×10^{-2}
β_0^m	6.41×10^{-3}
α_1^m	6.62×10^{-2}
β_1^m	9.65×10^{-2}
α_i^m	1.18×10^{-1}
β_i^m	1.21×10^{-1}
α_{i3}^m	2.32×10^{-3}
k_f	7.83×10^{-2}
k_b	5.80×10^{-2}

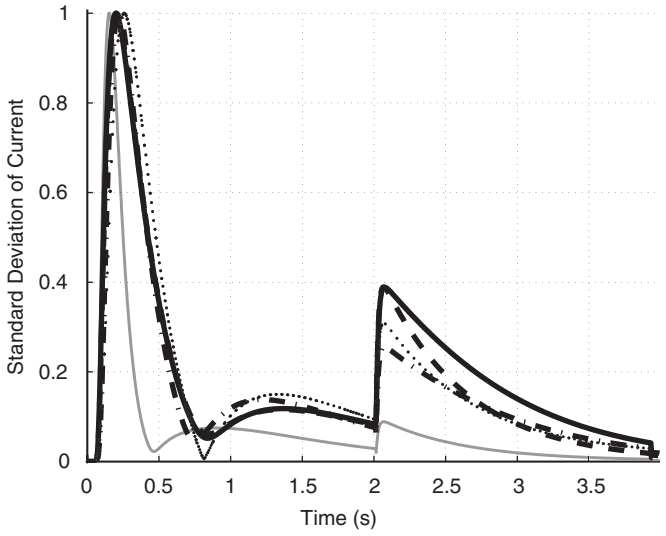

Fig. 5. Random α_0^m, β_0^m, α_1^m, k_f and k_b response to activation: the normalized standard deviation of the current is shown for random rate coefficients α_0^m (grey), β_0^m (solid), α_1^m (dotted), k_f (dashed), and k_b (dash-dotted), respectively. In each case, the rate coefficients have uniform distributions centered around their text values and ranging from ±50% of their mean value.

The standard deviation resulting from random rate coefficient multipliers, $\alpha_i^m(\xi)$ and $\beta_i^m(\xi)$, is depicted in Figs. 6 and 11. The standard deviations are unlike each other and different to standard deviations for the other stochastic rate coefficients. These parameter control the transitions between the open and inactivation states, and in the case of activation, have the highest maximum standard deviations of all the parameters studied. In the case of inactivation, $\beta_i^m(\xi)$, which controls the transition from the inactive to the open state, has the highest standard deviation. This effect is very brief and occurs at $t = 2$. The parameter $\alpha_i^m(\xi)$, which controls the rate of change from the open O to the inactive state I, has a less marked effect on the inactivation current response than both $\alpha_{i3}^m(\xi)$ and $\alpha_1^m(\xi)$.

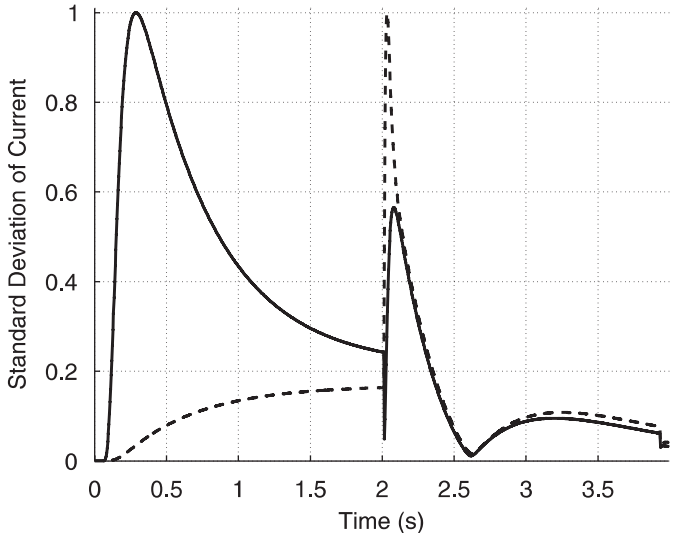

Fig. 6. Random α_i^m and β_i^m response to activation: the normalized standard deviation of the current is shown for random rate coefficients α_i^m (solid) and β_i^m (dashed). Maximum values are given in Table 5. In both cases, the rate coefficients have uniform distributions centered around their text values and ranging from ±50% of their mean value.

There are numerous possible permutations of rate coefficients, and SG can efficiently compute the standard deviations resulting from any of these combinations of random parameters. Due to space considerations, we only provide one instance here. Fig. 7 illustrates the different behavior as a result of perturbing both $\beta_1^m(\xi)$ and $k_f(\xi)$ as a function of the same random variable or two independent random variables. Though there is not a marked difference in the qualitative behavior in the I_{Kr} model, the latter case results in a slightly larger maximum standard deviation in the current between 2 and 3 s for the activation protocol (see also Figs. 8–11, Table 6).

4. Summary and conclusions

In this work a stochastic numerical technique based on Galerkin projections is introduced to extend and study Markovian models of ion channel electrophysiology. The generalized polynomial chaos stochastic Galerkin (gPC–SG) method allows one to take stochastic model parameters into account. We have demonstrated that gPC–SG is an efficient method of determining the effects of stochastic model parameters on the output of models. This information is beneficial in sensitivity analysis which has a number of potential applications, including model development and parameter tuning. Although slightly more complicated mathematically (from an implementation perspective) than standard Monte Carlo methods, this technique provides a computationally efficient means of modeling uncertainty.

The results of our exemplary studies with ion channel models indicate that rate coefficients modulate the standard deviation of electrical currents particularly after

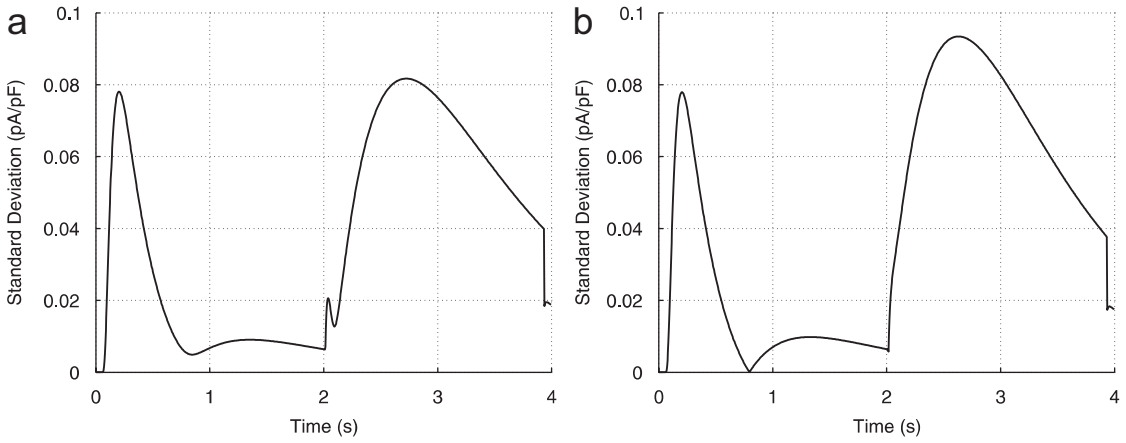

Fig. 7. Random β_1^m and k_f response to activation: these figures depict the standard deviation of the current response for I_{Kr} to the activation voltage clamping where both β_1^m and k_f have uniform distributions centered around the text value and range to ±50% of the mean values. (a) Both are functions of a single random variable. (b) Each is a function of two independent random variables.

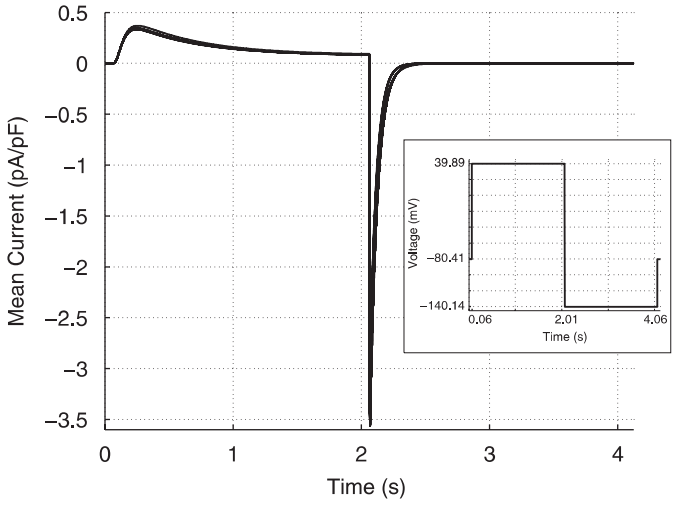

Fig. 8. I_{Kr} model response to inactivation: the current responses for all random experiments are shown together with the activation voltage clamping protocol (insert). The mean current for all random computational experiments were not significantly different from the deterministic response.

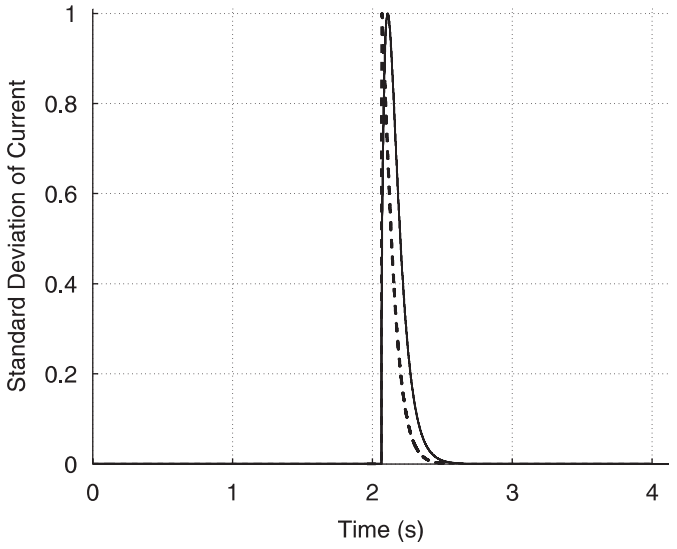

Fig. 9. Random β_1^m and α_{i3}^m response to inactivation: the normalized standard deviation of the current response is shown for random rate coefficients β_1^m (solid) and α_{i3}^m (dashed). In both cases, the coefficients have uniform distributions ranging from ±50% of their mean value. Maximum values for the standard deviations are given in Table 6.

voltage changes. This effect can also be observed in the study of uncertain rate coefficients $\alpha(\xi)$ and $\beta(\xi)$ in the simple model. Here, an increase of the standard deviation is obvious after the voltage step from −80 mV to −20 mV at $t = 2$ s (Fig. 2b). Asymptotic behavior of standard deviations to a constant value is observed in regions of constant clamping voltages. Further characterization of this behavior might show that the associated curve can be more accurately described as mono- or biexponential. Furthermore, in our study of the complex model we can identify groups of rate coefficients according to their impact on the standard deviation. Further analysis of this identification might help to characterize state transitions in complex stochastic Markovian models and ultimately to identify a reduced subset of states that achieve the necessary dynamics for the ion channels of interest.

In future work we will apply the technique to study stochastic fluctuations of ion channels and their impact on electrophysiology of cardiac cells. We will study current noise resulting from heterogeneity of kinetic channel properties and physical conditions in the channel vicinity. We expect that studies of channels mutations will profit from an application of the stochastic technique. The technique has potential to simplify prediction of electrophysiological consequences for heterozygous conditions of channels (Splawski et al., 2005), i.e. those are composed of

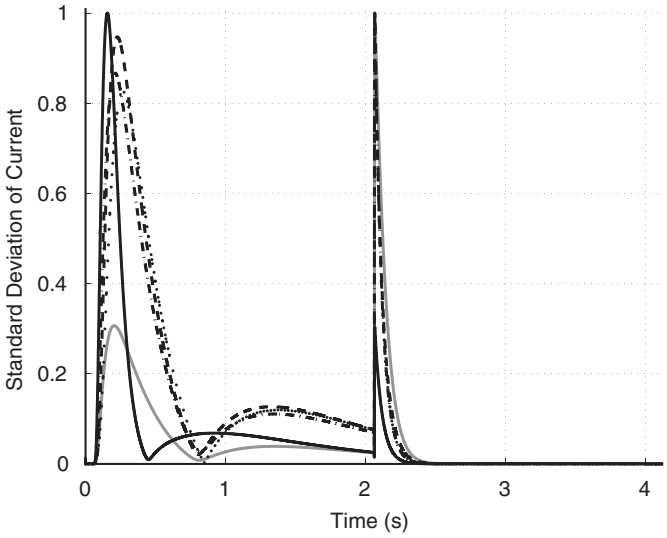

Fig. 10. Random α_0^m, β_0^m, α_1^m, k_f and k_b response to inactivation: the normalized standard deviation of the current response is shown for random rate coefficients α_0^m (solid), β_0^m (grey), α_1^m (dotted), k_f (dash-dotted), and k_b (dashed) respectively. In each case, the rate coefficients have uniform distributions ranging from ±50% of their mean value.

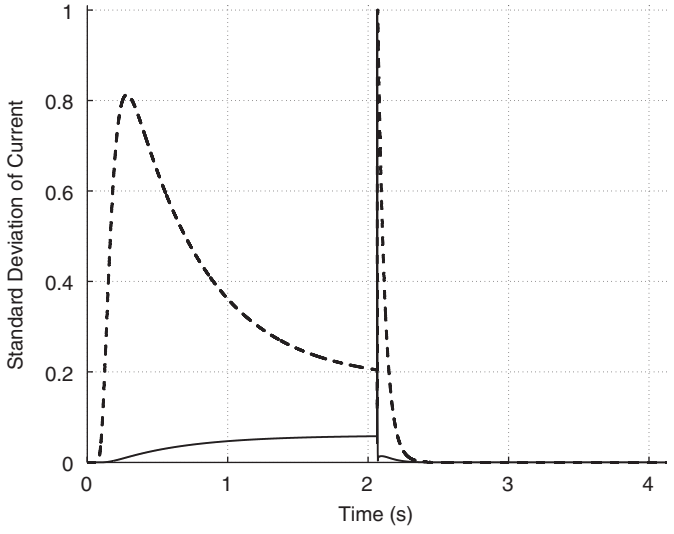

Fig. 11. Random α_i^m and β_i^m response to inactivation: these normalized standard deviation of the current is shown for random rate coefficients α_i^m (dashed), β_i^m (solid). Maximum values are given in Table 6. In both cases, the rate coefficients have uniform distributions ranging from ±50% of their mean value.

wild-type and mutated subunits and show heterogeneity of kinetic properties. Major steps to generate stochastic models will be the fitting of experimental data to the stochastic parameters and their validation. We propose that stochastic Galerkin methods could be used with an inverse solver to determine the model parameter probability distribution functions that generate the distributions of the system outputs observed experimentally.

Table 6
Maximum standard deviations of the current in response to random rate coefficients for inactivation protocol

Random rate coefficient	Maximum standard deviation
α_0^m	1.96×10^{-2}
β_0^m	4.00×10^{-3}
α_1^m	1.04×10^{-1}
β_1^m	1.98×10^{-1}
α_i^m	6.19×10^{-2}
β_i^m	1.78×10^{-1}
α_{i3}^m	6.75×10^{-2}
k_f	4.37×10^{-2}
k_b	2.88×10^{-2}

Acknowledgments

This work was funded in part by NSF Career Award (Kirby) NSF-CCF0347791, the NIH NCRR Center for Bioelectric Field Modeling, Simulation and Visualization (www.sci.utah.edu/ncrr), NIH NCRR Grant No. 5P41RR012553-02, the Richard A. and Nora Eccles Fund for Cardiovascular Research and awards from the Nora Eccles Treadwell Foundation (Sachse). The authors also acknowledge the computational support and resources provided by the Scientific Computing and Imaging Institute.

References

Canuto, C., Hussaini, M., Quarteroni, A., Zang, T., 1987. Spectral Methods in Fluid Mechanics. Springer, New York.

Colquhoun, D., Hawkes, A.G., 1995a. The principles of the stochastic interpretation of ion-channel mechanisms. In: Sakmann, B., Neher, E. (Eds.), Single Channel Recording, second ed. Plenum Press, New York, pp. 397–482 (Chapter 18).

Colquhoun, D., Hawkes, A.G., 1995b. How to write only one program to calculate the single-channel and macroscopic predictions for any kinetic mechanism. In: Sakmann, B., Neher, E. (Eds.), Single-Channel Recording, second ed. Plenum Press, New York, pp. 589–633 (Chapter 20).

Colquhoun, D., Sigworth, F.J., 1995. Fitting and statistical analysis of single-channel records. In: Sakmann, B., Neher, E. (Eds.), Single-Channel Recording, second ed. Plenum Press, New York, pp. 483–587 (Chapter 19).

Gamerman, L., 1997. Markov Chain Monte Carlo: Stochastic Simulation for Bayesian Inference. Chapman & Hall, London, England.

Ghanem, R., Spanos, P., 1991. Stochastic Finite Elements: A Spectral Approach. Springer, New York, NY.

Hairer, E., Norrsett, S.P., Wanner, G., 1993. Solving Ordinary Differential Equations I (2nd Revised ed.): Non-stiff Problems. Springer, New York, NY, USA.

Hille, B., 2001. Ion Channels of Excitable Membranes. Sinaure Associates, Inc., Sunderland, MA.

Hodgkin, A., Huxley, A., 1952. A quantitative description of membrane current and its application to conduction and excitation in nerve. J. Physiol. 11, 500–544.

Iyer, V., Mazhari, R., Winslow, R.L., 2004. A computational model of the human left-ventricular epicardial myocyte. Biophys. J. 87, 1507–1525.

Kleiber, M., Hein, T., 1992. The Stochastic Finite Element Method. Wiley, New York, NY, USA.

Liu, W., Belytschko, T., Mani, A., 1986. Random field finite elements. Internat. J. Numer. Meth. Eng. 23, 1831–1845.

Loh, W., 1996. On Latin hypercube sampling. Ann. Statist. 24, 2058–2080.

Luo, C.-H., Rudy, Y., 1991. A model of the ventricular cardiac action potential. Circ. Res. 68 (6), 1501–1526.

McAllister, R.E., Noble, D., Tsien, R.W., 1975. Reconstruction of the electrical activity of cardiac purkinje fibres. J. Physiol. 251, 1–59.

Niederreiter, H., Hellakalek, P., Larcher, G., Zinterhof, P., 1998. Monte Carlo and Quasi-Monte Carlo Methods. Springer, New York, NY, USA.

Rudy, Y., 2004. From genetics to cellular function using computational biology. Ann. N. Y. Acad. Sci. 1015, 261–270.

Sachse, F., 2004. Computational Cardiology: Modeling of Anatomy, Electrophysiology, and Mechanics. Lecture Notes in Computer Science, vol. 2966, Springer, Berlin, Heidelberg, New York.

Splawski, I., Timothy, K.W., Decher, N., Kumar, P., Sachse, F.B., Beggs, A.H., Sanguinetti, M.C., Keating, M.T., 2005. Severe arrhythmia disorder caused by cardiac l-type calcium channel mutations. Proc. Natl Acad. Sci. USA 102 (23), 8089–8096.

Verveen, A.A., DeFelice, L.J., 1974. Membrane noise. Prog. Biophys. Mol. Biol. 28, 189–265.

Wiener, N., 1938. The homogeneous chaos. Am. J. Math. 60, 897–936.

Xiu, D., Karniadakis, G., 2002a. The Wiener–Askey polynomial chaos for stochastic differential equations. SIAM J. Sci. Comput. 24 (2), 619–644.

Xiu, D., Karniadakis, G.E., 2002b. Modeling uncertainty in steady state diffusion problems via generalized polynomial chaos. Comput. Meth. Appl. Mech. Eng. 191 (43), 4927–4948.

Xiu, D., Karniadakis, G., 2003. Modeling uncertainty in flow simulations via generalized polynomial chaos. J. Comput. Phys. 187, 137–167.